Chinese Journal of
POLYMER SCIENCE

RESEARCH ARTICLE

https://doi.org/10.1007/s10118-026-3573-1
Chinese J. Polym. Sci. **2026**, *44*, 1790–1803

Nonlinear Stress Relaxation of End-associative Hydrophobically Modified Ethoxylated Urethane (HEUR) Solutions under Step Strain

Yu-Xuan Pei[a,b], Quan Chen[a,b*], and Hiroshi Watanabe[a,c*]

[a] *State Key Laboratory of Polymer Science and Technology, Changchun Institute of Applied Chemistry, Chinese Academy of Sciences, Changchun 130022, China*
[b] *School of Applied Chemistry and Engineering, University of Science and Technology of China, Hefei 230026, China*
[c] *Institute for Chemical Research, Kyoto University, Uji, Kyoto 611-0011, Japan*

Abstract Nonlinear stress relaxation under step strain γ was examined for aqueous solutions of an end-associative telechelic polymer, hydrophobically modified ethoxylated urethane (HEUR) having hexadecyl groups at the two ends of the chain. At 20 °C where the end hexadecyl groups were in the molten liquid state, the solutions with the HEUR concentrations c=1 wt% and 5 wt% commonly exhibited strain-hardening at short time t and the strain-softening (damping) at long t. In the terminal relaxation zone at sufficiently long t, the nonlinear relaxation modulus $G(t,\gamma)$ was found to obey the time-strain separability. These nonlinear features were discussed in relation to strain-induced changes in the associative network structure. In the aqueous HEUR solutions, aggregates of the precipitated end-groups should be stabilized by loops of dissolved HEUR backbones to form so-called flower micelles. At low c, most of those micelles would connect HEUR chains into a long linear sequence referred to as superbridge, thereby forming a sparse network. At higher c, those superbridges would become shorter to densify the network accordingly. Immediately after imposition of the large step strain, the flower micelles in the superbridge backbone would fuse each other to form a denser network thereby exhibiting the hardening. This micelle fusion would be more significant for longer superbridges to enhance the strain hardening at lower c. After this fusion, the micelles having liquid cores would be opened up because of the enhanced tension of the deformed superbridge, and then split to disconnect the superbridge if this tension overwhelms the micelle strength. This opening/splitting process possibly resulted in the partial breakage of the network and the corresponding softening. Finally, the surviving part of the network would relax on thermal dissociation of the remaining micelles thereby exhibiting the time-strain separable damping at long t. These features were semi-quantitatively described by a simple model that considered the strain-induced fusion followed by mechanical opening/breakage of the transient crosslinks.

Keywords Telechelic polymer; Nonlinear stress relaxation; Strain hardening; Strain softening; Time-strain separability

Citation: Pei, Y. X.; Chen, Q.; Watanabe, H. Nonlinear stress relaxation of end-associative hydrophobically modified ethoxylated urethane (HEUR) solutions under step strain. *Chinese J. Polym. Sci.* **2026**, *44*, 1790–1803.

INTRODUCTION

For aqueous (aq.) solutions of hydrophobically modified ethoxylated urethane (HEUR) end-capped with water-insoluble functional groups, rheological studies have been extensively conducted from experimental and theoretical points of view[1–20] because of the industrial importance of HEUR (for example, it has been used as a thickener in paints) as well as the scientific interest for a role of the association/dissociation dynamics of the end groups in rheological behavior. In general, the end groups such as alkyl groups precipitate in the aqueous solutions and associate with each other to form so-called flower micelles[1,2] being stabilized by loops of soluble chain backbones, as illustrated in Fig. 1. Those micelles exhibit thermal dissociation/association (unless the precipitated end groups are in the immobilized solid state) and can be also broken mechanically under large deformation. The thermal dissociation/association leads to linear viscoelastic relaxation whereas the mechanical breakage results in nonlinear rheological responses, as explained below in more detail.

The flower micelle serves as a connector at the chain ends to form linear sequences of the chain backbones, as discussed in the pioneering work by Annable and coworkers.[1,2] When those linear sequences are mutually overlapping in the solution, they are further organized into a network wherein three or more sequences are bound by one micelle (see Fig. 1). The linear sequence of the chain backbone incorporated in this network, referred to as superbridge,[1,2] sustains the network elasticity in a short time scale wherein the flower micelles at the middle/ends of the superbridge have experienced neither the thermally dissociation nor the mechanical breakage. At the same time, this network should include many defects such as a single-chain loop or a superloop[1,2] (not shown in Fig. 1, for simplicity), the latter being a loop of an end-connected sequence of the chain backbones. In addition, the solutions should also include isolated loops of various sizes not connected to the network. Thus, the HEUR solution includes various types of associated structures, which

* Corresponding authors, E-mail: qchen@ciac.ac.cn (Q.C.)
E-mail: hiroshi@scl.kyoto-u.ac.jp (H.W.)
Special Topic: Functional Gels
Received December 12, 2025; Accepted January 13, 2026; Published online March 20, 2026

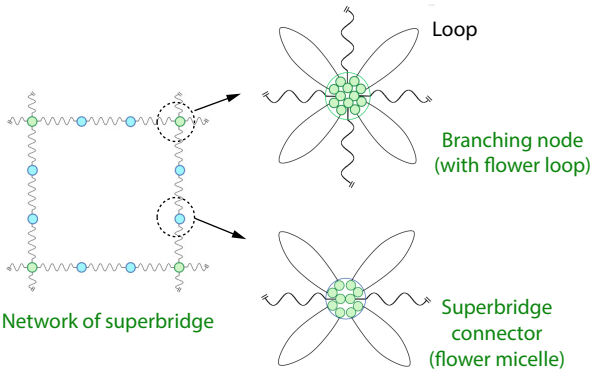

Fig. 1 Illustration of sparse network of HEUR superbridges dynamically crosslinked by flower micelles.

provides the solutions with rich rheological behavior, as summarized below.

Under small deformation, the flower micelles are not mechanically broken and their thermal dissociation/re-association governs the linear viscoelastic relaxation at long time. At low HEUR concentrations c below the overlapping concentration c^* of individual HEUR chains, the Maxwellian behavior characterized by the single relaxation time τ_M is experimentally observed and this τ_M has been assigned as the time required for the thermal dissociation of the flower micelles.[1–14] This relaxation broadens on an increase of c well above c^* possibly due to changes in the transient network structure, as discussed by Uneyama and coworkers:[13,14] A sparse network of the superbridges would be formed at low c so that the thermal dissociation resulting in the relaxation would dominantly occur at the micelles in the superbridge backbone, which naturally results in the single-τ_M relaxation (because motion of the cleaved superbridge is much faster than the thermal dissociation). The transient network model of Tanaka and Edwards[16] can capture this feature of linear viscoelastic relaxation. In contrast, at high c, a dense network would be formed so that the relaxation would be *also* contributed from the thermal cleavage of the transient network junctions (branching nodes shown in Fig. 1) and become broadened.[13,14]

Under large deformation/fast flow, the flower micelles can be mechanically broken to provide the solutions with even richer rheological behavior, the shear thickening of the steady state viscosity η at the shear rate $\dot{\gamma}\sim1/\tau_M$ followed by the thinning of η at $\dot{\gamma} > 1/\tau_M$.[4–12] Ma and Cooper,[8] Berret and coworkers,[6,7] and Pellens and coworkers[9–11] attributed the thickening to the finite-extensive nonlinear elasticity (FENE) of those strands modelled by Marrucci and coworkers.[15] In contrast, Tam and coworkers[4,5] attributed the thickening to a flow-induced increase of the number density ν_{sb} of the superbridges (occurring through fusion of the micelles in the backbone of the superbridges, for example). Tanaka, Koga, Indei, and coworkers[16–20] formulated a transient network model considering the FENE effect as well as the increase of ν_{sb}. Nevertheless, Suzuki and coworkers[14] experimentally found that the first normal stress difference coefficient Ψ_1 of a low-c HEUR solution keeps its linear viscoelastic value even when η exhibits the thickening at $\dot{\gamma}\sim1/\tau_M$. This behavior of Ψ_1 is not expected from the simple ideas of FENE and flow-induced increase of ν_{sb}. For this problem, Uneyama, Suzuki, and coworkers[12,13] proposed a model considering that the superbridges disrupted under flow are reformed anisotropically thereby leading to the above-mentioned difference between the Ψ_1 and η data. Furthermore, they found that the difference between the nonlinearities of Ψ_1 and η becomes minor (no thickening for both η and Ψ_1) in the solutions at high c wherein the dense network of the HEUR chains, not of the superbridges, are formed.

Here, we realize that HEUR is situated in a wider class of telechelic polymers having associative end groups, for example, hydrogen bonding groups[21–25] and ionic salt groups.[26–31] It is of interest to examine if the rheological behavior of the HEUR solution is similar to that of the telechelic polymers in general, or, if a difference is noted according to the difference in the strength of the associative interaction of the end groups. For this point, we remember our recent study[31] for a polystyrene ionomer (SPS-Na) having two sodium sulfonate salt groups *per* chain on average. This ionomer can be regarded as a telechelic chain strongly associating through the coulombic interaction between the salt groups. Our nonlinear relaxation experiments revealed that the SPS-Na ionomer shows the strain-hardening at short t and the time-strain separable strain-softening (damping) at long t, attributable to strain-induced fusion of the salt aggregates at short t followed by mechanical rupture and thermal dissociation of those aggregates at long t. It is of interest to examine if the HEUR aq. solution exhibits similar hardening and softening behavior. If this similarity is observed, we can discuss factors that determine the magnitudes of the hardening and softening.

On the basis of this consideration, we focused on model HEUR aq. solutions at low and high c (1 wt% and 5 wt%) and tested their nonlinear behavior *under step shear* (not examined in previous studies by Uneyama, Suzuki, and coworkers[12,13]). Those solutions were found to exhibit the hardening at short t and time-strain separable softening at long t, which was qualitatively similar to the SPS-Na ionomer. In addition, a simple model for the magnitudes of hardening and softening, extended from a model for the ionomers,[31] was able to approximately describe those magnitudes observed for the HEUR solutions. These results allowed us to situate the short-t hardening and long-t softening as general features of telechelic associative polymers. Furthermore, the difference in the magnitudes of long-t softening of the HEUR solutions and the SPS-Na ionomer defined with respect to the short-t hardening (the softening defined in this way being much weaker for the HEUR solutions) suggested that the ductility of the associating groups plays an important role of the nonlinear behavior of telechelic polymers, which enabled us to extend the previous view[12,13,31] for the nonlinearity. Details of these results are presented in this work.

EXPERIMENTAL

Materials

The hydrophobically modified ethoxylated urethane (HEUR) sample used in this study was synthesized and characterized by Suzuki and coworkers,[12] and had hexadecyl end groups as shown in Fig. 2. Its weight-average molecular weight and polydispersity index were M_w=4.6×10^4 g·mol^{-1} and M_w/M_n=1.35, respectively.[12]

Aqueous HEUR solutions with concentrations of 1 wt% and 5 wt% were prepared by dissolving prescribed amounts of the HEUR sample in distilled water. To ensure homogeneity of the solutions, the HEUE/water mixtures were stirred continuously at 40 °C for 24 h in sealed containers prior to rheological tests.

Measurements

Dynamic measurements of the storage and loss moduli $G'(\omega)$ and $G''(\omega)$ in the linear viscoelastic (LVE) regime and stress relaxation measurements under step strain were conducted with a strain controlled rheometer (ARES-G2, TA Instruments) at 20 (±1) °C for the 1 wt% and 5 wt% aqueous solutions of HEUR. A cone-and-plate fixture of 25 mm diameter, 2.3° cone angle, and 0.0539 mm truncation gap was used. All measurements were made in a saturated humidity atmosphere to prevent water (solvent) evaporation from the sample solutions. In the stress relaxation measurements, the sample was subjected to a step strain γ in a range between 0.5 and 10. Before those measurements at each γ, we tested the reproducibility of the $G'(\omega)$ and $G''(\omega)$ data and confirmed lack of changes in the solution samples (due to water evaporation, for example).

RESULTS AND DISCUSSION

Linear Viscoelastic Behavior

For the 1 wt% and 5 wt% HEUR solutions at 20 °C, Fig. 3(a) presents data of the storage and loss modulus, $G'(\omega)$ and $G''(\omega)$ (filled and unfilled symbols), measured as functions of angular frequency ω. Those data allow us to evaluate the terminal relaxation time $\tau = [G'/\omega^2]_{\omega\to 0}/[G''/\omega]_{\omega\to 0}$ and the plateau modulus G_{pl}, the latter emerging at ω well above $1/\tau$ and characterizing the intensity of terminal relaxation. The results are summarized in Table 1. The terminal relaxation is fully covered in our experimental window, which allows us to systematically investigate the nonlinear rheological behavior in the relevant timescales as explained later.

The plateau modulus $G°$ of fully developed dense network of individual HEUR chains is specified as

$$G° = \frac{cRT}{M_{HEUR}} \quad (1)$$

where $M_{HEUR}=M_{n,HEUR}=3.4\times10^4$ g·mol^{-1}, c represents the mass concentration of the solution, R is the gas constant, and T stands for the absolute temperature. This $G°$ is shown by the horizontal dotted lines in Fig. 3(a). For the HEUR solutions with c=1 wt% and 5 wt%, respectively, the measured plateau modulus G_{pl} is only 1/42 and 1/7 of this $G°$, suggesting that the transient network in the HEUR solutions, in particular in the 1 wt% solution, is mainly sustained by the superbridges of the HEUR chain. Namely, the dense (and perfect) network of individual HEUR chains was formed neither at c=1 wt% nor at c=5 wt%. This result agrees with that reported by Uneyama and coworkers.[13]

The relaxation mode distribution of the two HEUR solutions can be most straightforwardly compared for the storage and loss moduli reduced by the plateau modulus, G'/G_{pl} and G''/G_{pl}, and plotted against the normalized frequency $\omega\tau$.

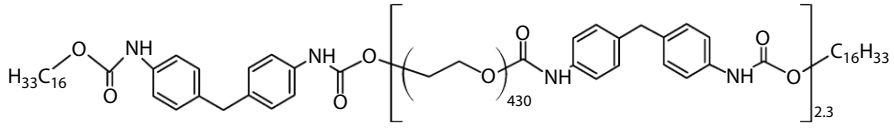

Fig. 2 Chemical structure of HEUR chain used in this study.

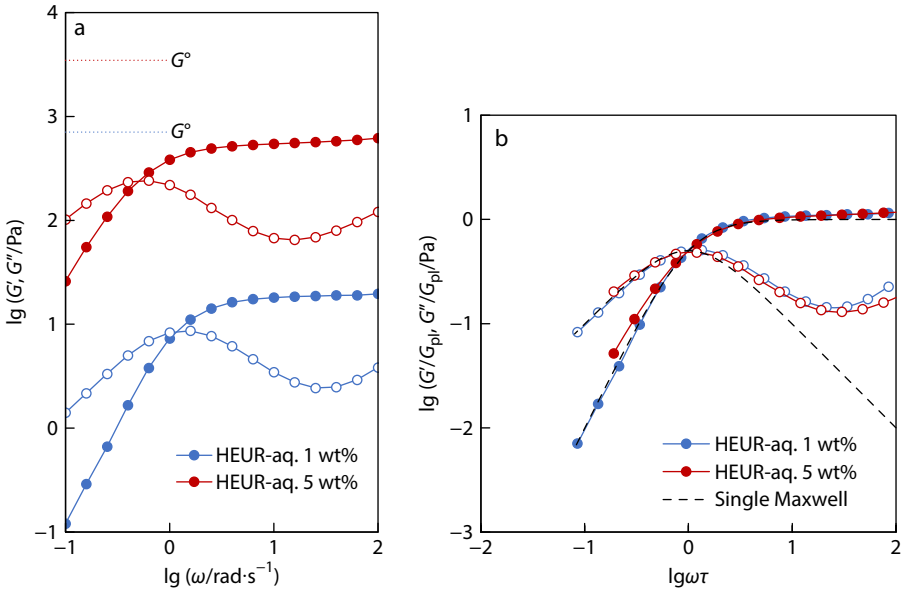

Fig. 3 (a) Linear viscoelastic moduli G' (filled circles) and G'' (unfilled circles) at 20 °C obtained for the 1 wt% and 5 wt% HEUR solutions. $G°$ represents the nominal plateau modulus expected for an ideally dense network of HEUR chains. (b) Normalized plots of the data shown in panel (a). The moduli data reduced by the measured plateau modulus G_{pl} are plotted against the angular frequency normalized by the terminal relaxation frequency $1/\tau$. The black dotted curves indicate the result of fitting the $G'(\omega)$ and $G''(\omega)$ data with the single-Maxwell model.

https://doi.org/10.1007/s10118-026-3573-1

Table 1 τ and G_{pl} values of the 1 wt % and 5 wt % HEUR solutions at 20 °C.

c_{HEUR}	τ (s)	G_{pl} (Pa)
1 wt%	0.8	17
5 wt%	2.5	500

The results are shown in Fig. 3(b). At low $\omega\tau$, both solutions exhibit the terminal relaxation similar to the Maxwellian relaxation, $G'/G_{pl} = \omega^2\tau^2/(1 + \omega^2\tau^2)$ and $G''/G_{pl} = \omega\tau/(1 + \omega^2\tau^2)$, shown with the dotted curve. This terminal relaxation is attributable to the thermal dissociation of the flower micelles in the superbridge backbone.[13] Correspondingly, the upturn of G''/G_{pl} and the corresponding gradual increase of G'/G_{pl} seen at $\omega\tau \geq 10$ is attributable to the motion of the superbridges before occurrence of this thermal dissociation.

In Fig. 3(b), a close inspection of G'/G_{pl} data at $\omega\tau<1$ suggests that the terminal relaxation of the HEUR solution is slightly broader for c=5 wt% than for c=1 wt%. This behavior, noted also by Uneyama and coworkers,[13] can be assigned as the crossover in the transient network structure from the sparse network to the dense network. In fact, a considerably broader terminal relaxation mode distribution characterizing this crossover has been noted at c=10 wt%.[13]

Nonlinear Stress Relaxation

Fig. 4 compares the relaxation modulus $G(t,\gamma)$ under various step strains γ measured for the HEUR solutions with c=1 wt% and 5 wt% at T=20 °C. The black dashed curve indicates the linear viscoelastic $G(t)$ calculated from the G' and G'' data in Fig. 3(a). For both 1 wt% and 5 wt% solutions, $G(t,\gamma)$ for $\gamma \leq 1$ agrees with this $G(t)$ and exhibits the LVE plateau noted in Fig. 3(a). However, an increase of γ results in a significant deviation of $G(t,\gamma)$ from $G(t)$, namely, strong nonlinearity.

At very short t, $G(t,\gamma)$ increases with increasing γ for both samples, and this increase (strain-hardening) is stronger for the 1 wt% solution than for the 5 wt% solution. At short t after the hardening, $G(t,\gamma)$ exhibits a rapid decay when the strain exceeds a certain value, γ =7 and 5 for c=1 wt% and 5 wt%, respectively. This decay becomes faster with an increase of γ. Irrespective of γ, $G(t,\gamma)$ at long t fully relaxes with a rate similar to that for $G(t)$. These two major characteristics, the strain-hardening and strain-softening being qualitatively similar to those observed for SPS-Na ionomer,[31] are examined below in more detail.

Strain-hardening

Under large step strains, the HEUR solutions and SPS-Na ionomer, the latter examined in our previous study,[31] commonly exhibit hardening at short t. However, this hardening is quantitatively different for these two associative systems. For the SPS-Na ionomers under moderate γ (still below 2), $G(t,\gamma)$ at short-t increased almost up to the ideal modulus $G°$. This behavior suggests that the strain induces collision and fusion of the salt aggregates in the SPS backbone of neighboring superbridges, thereby converting the associative network in the SPS-Na ionomer to an almost defect-free network of the SPS backbone between the two sodium sulfonate salt groups therein. Consequently, the nonlinear damping of this ionomer at long t would reflect the strain-induced rupture of this almost defect-free network. In contrast, for the HEUR solutions with c=1 wt% and 5 wt%, the short-t modulus increases only to a level well below $G°$ even under the very large strain, γ =10 (*cf.* Fig. 4). This result suggests that the nonlinear damping of those HEUR solutions at long t reflects strain-induced structure changes of the sparse network containing many defects, possibly the network effectively composed of superbridges carrying flower micelles (*cf.* Fig. 1).

This point can be further examined in relation to the magnitude of overlapping between HEUR chains in the unassociated state. We may roughly estimate the overlapping concentration c^* of the HEUR chain in that state from the intrinsic viscosity $[\eta]$ of the poly(ethylene oxide) (PEO) sequence included in the HEUR backbone as the main component. (The urethane and hexadecyl groups are not soluble in water and

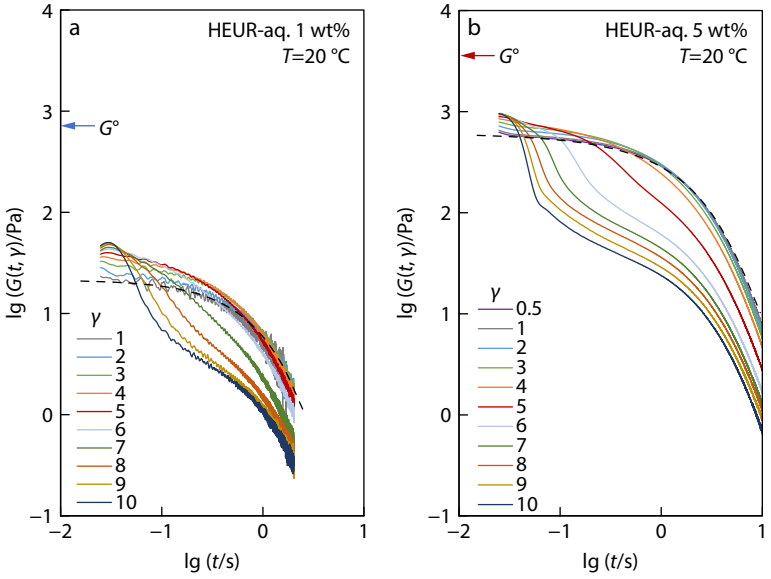

Fig. 4 Nonlinear relaxation modulus $G(t,\gamma)$ of the HEUR solutions with (a) c=1 wt% and (b) c=5 wt% at T=20 °C. The dashed curves show linear viscoelastic $G(t)$ calculated from the G' and G'' data in Fig. 3(a). $G°$ represents the ideal modulus specified by Eq. (1).

would not contribute to [η] in the unassociated state.) From the molecular weight of this PEO sequence, $M_{PEO} \cong 44\times430\times2.3=4.3\times10^4$ g·mol^{-1} (*cf.* Fig. 2), an empirical equation reported for PEO in water at 25 °C,[32] $[\eta]_{PEO} = 4.33\times10^{-4}M_{PEO}^{0.679}$ g^{-1}·dL, and the mass densities $d_{water} \cong d_{PEO} \cong 1$ g·cm^{-3}, we obtain an estimate for our HEUR chain, $c^* \cong 1/[\eta]_{PEO} \cong 1.6$ g·dL^{-1} $\cong$ 1.6 wt%, under an assumption of no volume change on mixing. As judged from this c^* value, the HEUR chains in the 1 wt% solution ($c/c^* \cong 0.6$) are not in the overlapping state unless they associate with each other, and their associated network should have included many defects even in the strain-hardened state (where $G(t,\gamma)$ at short t is much smaller than $G°$; *cf.* Fig. 4). In contrast, some overlapping is expected for the HEUR chains in the 5 wt% solution ($c/c^* \cong 3.1$) even in the unassociated state. Nevertheless, the associated network in this solution should still include considerable defects, as judged from its hardened $G(t,\gamma)$ still smaller than $G°$ (*cf.* Fig. 4). This imperfectness of the associated network in the 5 wt% solution can be also deduced in Fig. 6 of Ref. [13]: The LVE plateau modulus of the 5 wt% solution is located only at the low-c end of a high-c asymptotic power-law zone for the well-developed network.

In relation to the above argument, it is informative to examine if the PS chain backbones of the SPS-Na ionomer melt are well overlapping with each other. Utilizing an empirical equation for PS in a theta solvent, cyclohexane (CH) at 34.5 °C,[33] $[\eta]_{PS} = 85.7\times10^{-3}M_{PS}^{0.5}$ g^{-1}·dL, the ionomer molecular weight[31] $M_{SPS}=1.1\times10^4$ g·mol^{-1}, and the mass densities $d_{CH} \cong 0.78$ g·cm^{-3} and $d_{PS} \cong 1.05$ g·cm^{-3}, we can estimate a hypothetical intrinsic viscosity of unassociated SPS in the theta state and the corresponding overlapping concentration, $[\eta]_{SPS} = 9.0$ g^{-1}·cm^3 and $c^* = 1/[\eta]_{SPS} = 0.11$ g·cm^{-3} $\cong$ 13 wt%. Thus, SPS-Na chains in melt (c=100 wt%, $c/c^* \cong 7.7$) are in a more heavily overlapping state compared to the HEUR chains in the solutions with c=1 wt% and 5 wt%. Nevertheless, the associated network in the SPS-Na ionomer melt still includes defects, as discussed previously in relation to its hardening behavior.[31]

On the basis of the above consideration for defects in the associative network, detailed features of the hardening of the HEUR solutions at very short t are examined in Fig. 5 where the $G(t,\gamma)$ data are reduced by a hardening factor $\tilde{h}(\gamma)(\geq1)$. The gray curve shows the raw $G(t,\gamma)$ data for γ=1, *i.e.*, $G(t)$ in the LVE regime. For all $\gamma>1$, $\tilde{h}(\gamma)$ was determined by superposing the short-t plateau in the hardening zone onto the LVE plateau, namely $\tilde{h}(\gamma) \equiv G(t,\gamma)/G(t,1)$ at the shortest time (t=0.03 s) required for accurate measurement of $G(t,\gamma)$. For the SPS-Na ionomer, $\tilde{h}(\gamma)$ defined in this way reflects strain-induced enhancement of the network association at such short t.[31] This is the case also for the HEUR solutions.

The $\tilde{h}(\gamma)$ factors thus evaluated are summarized in Fig. 6(a). Another factor characterizing the short-t behavior, $G°/G(0,\gamma)$ defined with respect to $G°$ of fully developed dense network, is shown in Fig. 6(b). For comparison, the data of SPS-Na obtained in our previous study[31] are also shown. Comparing the behavior of two HEUR solutions with c=1 wt% and 5 wt%, we note that the hardening is stronger and the $G°/G(0,\gamma)$ factor is larger (defects in the transient network remains more even in the hardened state) for the former solution. At the same time, the hardening of the two HEUR solutions is considerably weaker and their $G°/G(0,\gamma)$ ratio is larger (defects remain more) compared to the SPS-Na ionomer. This difference between the HEUR solutions and the SPS-Na ionomer provides us with a clue for discussing the structural origin of the hardening.

Strain-softening

Fig. 7 shows plots of the $G(t,\gamma)$ data of the two HEUR solutions reduced by respective damping functions $h(\gamma)$. With an adequate choice of $h(\gamma)$ shown in Fig. 8, the reduced $G(t,\gamma)/h(\gamma)$ data of respective HEUR solutions are excellently superposed on the LVE $G(t)$ data (gray curve) at long t, as noted in Fig. 7. Namely, the slow relaxation of the HEUR solutions satisfies the time-strain separability:

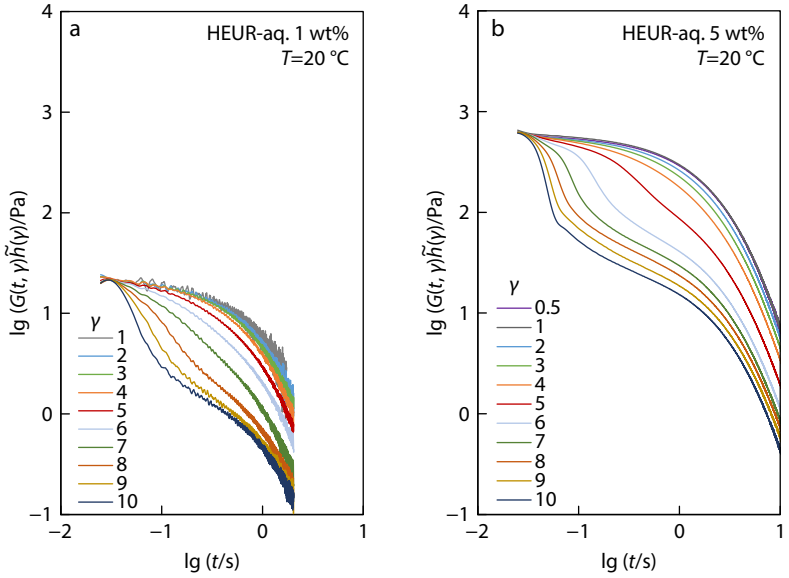

Fig. 5 Comparison of hardening behavior of the HEUR solutions with (a) c=1 wt% and (b) c=5 wt%.

https://doi.org/10.1007/s10118-026-3573-1

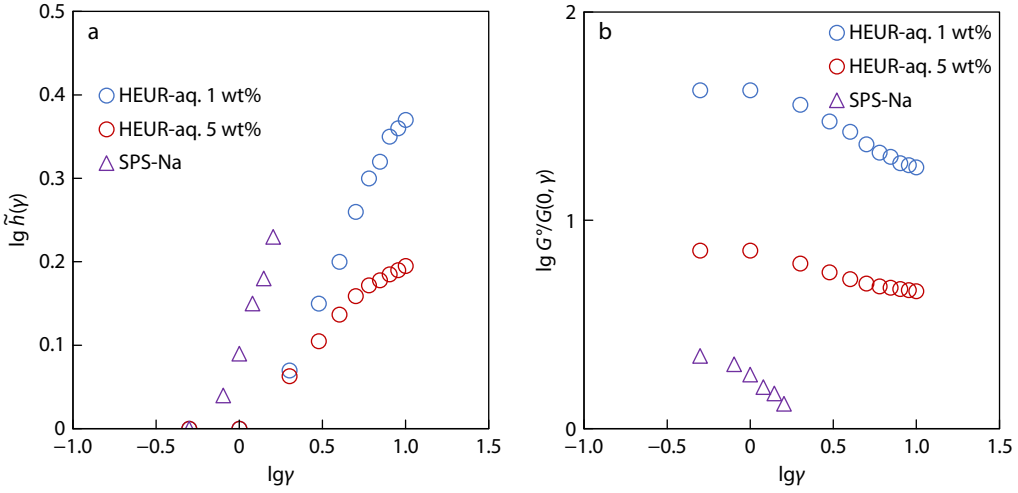

Fig. 6 Short time nonlinearity of the c=1 wt% and 5 wt% HEUR solutions at T=20 °C. For comparison, the data of SPS-Na[31] are also shown. (a) Hardening factor $\tilde{h}(\gamma)$ double-logarithmically plotted against γ. (b) $G^\circ/G(0,\gamma)$ ratio defined with respect to G° of fully developed dense network.

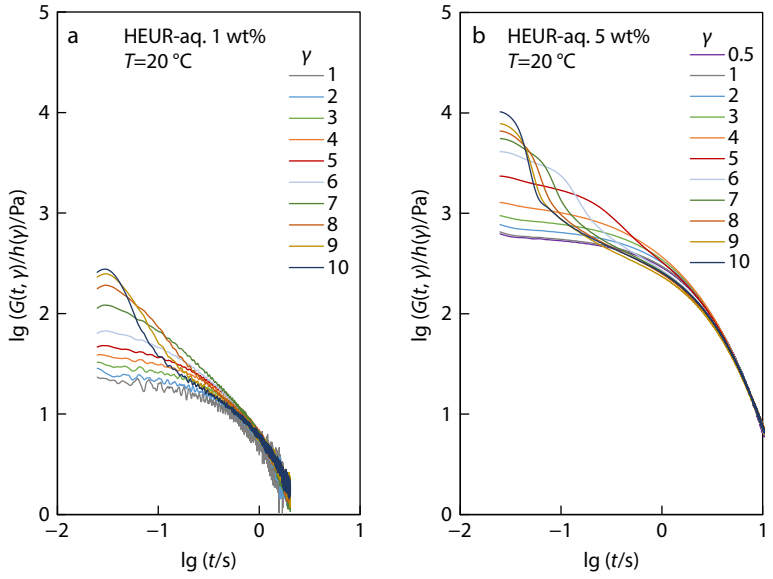

Fig. 7 Test of time-strain separability of (a) 1 wt% and (b) 5 wt% HEUR solutions at long t.

$$G(t,\gamma) = G(t)h(\gamma) \text{ at long } t \quad (2)$$

This separability is observed also for entangled linear polymers[34] and SPS-Na ionomer.[31] Nevertheless, the damping function of the HEUR solutions is less dependent on γ compared to the entangled linear polymers and SPS-Na ionomer, as clearly noted in Fig. 8. We also note that the damping from the LVE behavior is stronger ($h(\gamma)$ is smaller) for the 5 wt% HEUR solution than for the 1 wt% solution.

Here, we should note that the two HEUR solutions exhibit an enhanced plateau of the modulus (strain-hardening) at short t; *cf*. Fig. 4. Thus, for these solutions, the decrease of the terminal relaxation intensity with γ is better defined as a decrease from this short-t plateau and is quantified by an effective damping function, $h_{\text{eff}}(\gamma) = h(\gamma)/\tilde{h}(\gamma)$ with $\tilde{h}(\gamma)$ (≥1) being the hardening factor examined in Fig. 6. For the two HEUR solutions, Fig. 9 shows changes of $h_{\text{eff}}(\gamma)$ with γ. For comparison, the results for the SPS-Na ionomer[31] are also shown. The differences between the two HEUR solutions seen in Fig. 8 becomes less significant in Fig. 9, although the difference of $h_{\text{eff}}(\gamma)$ for c=1 wt% and 5 wt% is still detectable ($h_{\text{eff}}(\gamma)$ is a little larger for c=1 wt%). Furthermore, the large difference between the solutions and the ionomer still remains in Fig. 9. These observations are later discussed in relation to results of a model analysis considering a strain-induced structure change of the associative network followed by re-association in a partially relaxed form.

Mechanism of Strain-hardening at Short Time

For HEUR solutions, Suzuki and coworkers[12] observed shear thickening of the steady state viscosity η but not of the first normal stress difference coefficient Ψ_1. This observation led them to rule out the FENE effect and a simple flow-induced enhancement of association (both increasing η and Ψ_1 to the same magnitude) as the molecular origin of the thickening observed just for η. Consequently, they attributed the thickening of the HEUR solutions to anisotropic reorganization of the transient network under flow: Specifically, they focused on the averaged

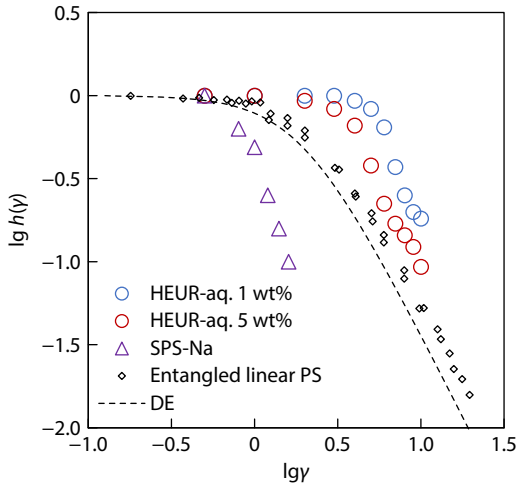

Fig. 8 Damping function $h(\gamma)$ of 1 wt% and 5 wt% HEUR solutions obtained from the shift of the $G(t,\gamma)$ data shown in Fig. 7. For comparison, the damping function is shown also for the SPS-Na ionomer and entangled linear polystyrene (PS). The dotted curve shows the prediction of the Doi-Edward (DE) model for entangled polymers. The data for PS and SPS-Na and the DE curve were taken from Ref. [31] with a permission of American Chemical Society (Order Number 6142240716763).

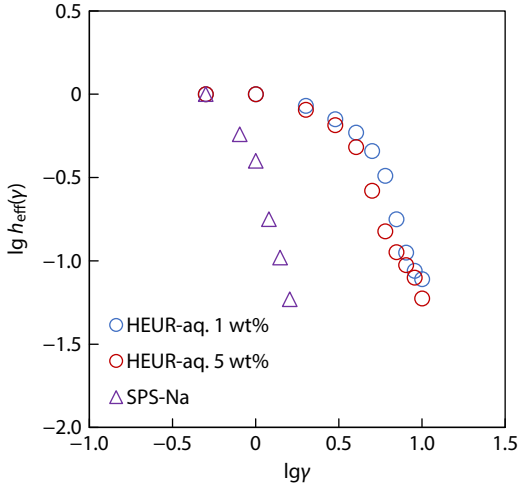

Fig. 9 Effective damping function $h_{\text{eff}}(\gamma) = h(\gamma)/\tilde{h}(\gamma)$ of HEUR solutions with c=1 wt% and 5 wt%. $h_{\text{eff}}(\gamma)$ quantifies the damping at long t with respect to the strain-hardened state at short t. For comparison, $h_{\text{eff}}(\gamma)$ data of the SPS-Na ionomer[31] are also shown.

dyadic $\langle \mathbf{rr} \rangle$ of the end-to-end vector $\mathbf{r}$ of the network strands and argued that the reorganization occurred in a direction enhancing the dyadic component $\langle r_x r_y \rangle$ ($\sim \eta\dot{\gamma}$) but not affecting $\langle r_x^2 - r_y^2 \rangle$ ($\sim \Psi_1 \dot{\gamma}^2$), with x and y being the shear and shear gradient directions, respectively.

Considering the above argument of Suzuki and coworkers,[12] we examine a structural origin of the strain-hardening of our HEUR solutions observed under step strain at short t (in a sense similar to the thickening of η explained above). Specifically, we firstly test the FENE effect and then the network reorganization (fusion of the flower micelles located in the superbridge backbone) as a mechanism underlying the observed hardening.

Test of FENE effect

As a test of the FENE mechanism, we conducted a double-step relaxation experiment illustrated in Fig. 10. We applied a large positive step strain γ_1=3 to the 1 wt% and 5 wt% HEUR solutions at time $t = -t_w$ and then applied a negative strain of the same magnitude, γ_2=−3, at time t=0. The interval between these two strains, t_w=0.1 s, was chosen to be much shorter than the time required for the strain-hardened plateau of $G(t,\gamma)$ to start decaying (for γ=3, this decay starts at $t \cong 0.8$ and 2.5 s for the 1 wt% and 5 wt% solutions; *cf.* Fig. 4). In this condition, the HEUR solutions should behave as a chemically crosslinked rubber and exhibit practically zero stress at t>0 given that their associative network structure is unaffected by the strain and the hardening is mainly due to the FENE effect.

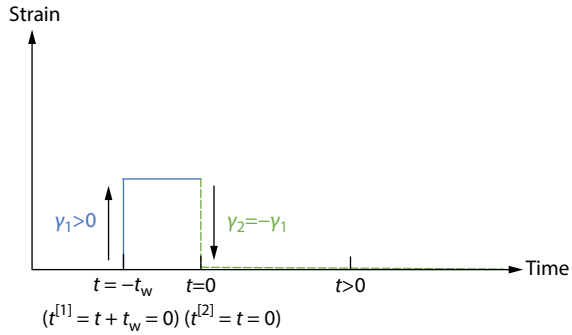

Fig. 10 Schematic illustration of double-step strain test. A positive strain γ_1 (=3) was applied at a time $t = -t_w$, and a negative strain of the same magnitude was applied at time t=0. The stress of the HEUR samples were measured in the whole process of this test.

Fig. 11 shows the results of this double-step strain test. Under the first strain, both 1 wt% and 5 wt% HEUR solutions exhibited a positive stress $\sigma^{[1]}$ that hardly decayed within the interval time, 0.1 s. Under the second step strain, both samples exhibited a negative stress $\sigma^{[2]}$ of large magnitude. This result unequivocally rules out the possibility of the FENE mechanism as the main mechanism for the strain hardening of our HEUR solutions.

Strain-induced fusion of flower micelles

The above test rules out the FENE effect as the primary mechanism for the short-t strain hardening of the HEUR solutions. Thus, we propose that the hardening observed under the step strain is primarily due to strain-induced fusion of flower micelles in the superbridges. We may consider that the associative networks formed in our HEUR solutions consist mainly of superbridges, in particular in the 1 wt% solution, as illustrated in Fig. 1. In this network, the aggregates of $C_{16}H_{33}$ alkyl groups at the ends of the superbridges serve as the branching nodes of the network. This node is stabilized by the loops that protect the hydrophobic alkyl aggregates from the aqueous phase. The flower micelles in the superbridge backbone are also protected by the loops.

In the HEUR solution with c=1 wt% (well below the overlap concentration of the HEUR chains estimated earlier, $c^* \cong 1.6$ wt%), the superbridges appear to behave as effective strands forming a sparse network. Upon application of step strain, the micelles within the superbridge backbone would undergo fusion, which leads to network densification and consequently

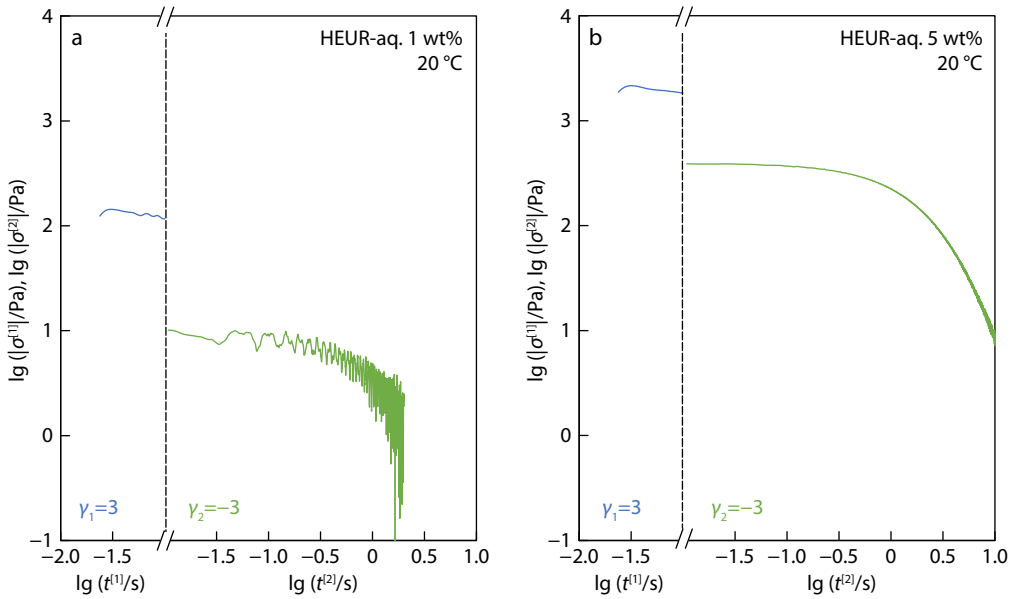

Fig. 11 Plots of shear stress σ measured for the (a) 1 wt% and (b) 5 wt% HEUR solutions under the double step strain. For both solutions, $\sigma^{[1]}$ and $\sigma^{[2]}$ under the first and second step strains were of positive and negative values, respectively.

pronounced strain hardening. In contrast, in the HEUR solution with c=5 wt% (moderately larger than c^*), the network should be denser and the superbridges may become minor, which would reduce a probability of flower micelle fusion and thus give rise to only moderate hardening.

It is worth noting that the aggregates of $C_{16}H_{33}$ alkyl groups are in a molten liquid state at 20 °C, as judged from the melting temperature T_{melt}=18 °C of pure $C_{16}H_{34}$ (hexadecane). Therefore, on application of a large step strain, these soft domains would be fused to activate the hardening seen in Fig. 4, and then deformed and finally cleaved to exhibit the softening at long t. This liquid feature of the $C_{16}H_{33}$ group makes a contrast to a solid feature of the sodium sulfonate salt aggregates in the SPS-Na ionomer examined previously.[31] The fusion would have occurred less significantly and the hardening would have been weaker for those solid aggregates compared to the liquid $C_{16}H_{33}$ groups if the defect content in the network at equilibrium were similar for the SPS-Na ionomer and the HEUR solutions. However, the strong electrostatic attraction between the salt aggregates should have resulted in a denser transient network at equilibrium compared to that in the HEUR solutions formed through a rather weak hydrophobic interaction of the alkyl groups. This difference between the ionomer and HEUR solutions naturally resulted in differences noted in Fig. 6, the hardening occurring at smaller γ (larger $\tilde{h}(\gamma)$ at a given γ) but in a narrower range of the modulus (smaller $G°/G(0,\gamma)$ ratio) noted for the ionomer.

Magnitude of time-strain separable damping at long time

The HEUR network in the strain-hardened state is deformed and thus its structure will further change over time. Fig. 12 illustrates those changes expected for the network strand, *i.e.*, the deformed/stretched superbridge after the flower-micelle fusion (in the strain-hardened state; *cf.* Fig. 12a). For this superbridge, we expect two types of structure change: A flower micelle may split into two smaller flower micelles that are either connected by the HEUR backbone (Fig. 12b) or fully disconnected (Fig. 12c). In the former case, the superbridge becomes longer but still connects the network nodes thereby being oriented/deformed to sustain the shear stress. In the latter case, the superbridge is broken into two shorter tails, which results in full relaxation of the stress.

This dual structural changes in the HEUR solutions should be related to the feature of aggregates of the alkyl groups. At 20 °C, these aggregates are in the liquid state and would easily deform on application of the step strain, which enables the flower micelle to split into *mutually connected* smaller micelles (*cf.* Fig. 12b). In this sense, the alkyl aggregates in the HEUR solution can be regarded as ductile aggregates that can still sustain the stress after splitting. In the next section, we consider the dual structural changes shown in Fig. 12 to conduct model analysis of the softening of the HEUR solutions at long t. (In relation to this point, we should add that the salt aggregates in SPS-Na ionomer formed through the coulombic attraction cannot easily change its shape and are expected to behave as fragile aggregates. Thus, in the modelling for the ionomer,[31] we just considered the superbridge cessation shown in Fig. 12c.)

Model Analysis

For the HEUR solutions, we focus on the effective damping function $h_{eff}(\gamma) = h(\gamma)/\tilde{h}(\gamma)$ describing the damping from the starin-hardened state at short t (*cf.* Fig. 9). This $h_{eff}(\gamma)$ reflects the structural changes of the transient network after the strain-induced fusion of the flower micelles in the superbridge backbone (in the strain-hardened state).

For analysis of $h_{eff}(\gamma)$, we consider a superbridge having N + 1 HEUR chains in its backbone just after the micelle fusion (Fig. 12a). This superbridge backbone carries N flower micelles containing the aggregates of alkyl groups of the HEUR chains. The superbridge is *assumed* to be affinely deformed with respect to the step strain, and then n flower micelles (n=0, 1, ..., N) may open to release n HEUR chains into the su-

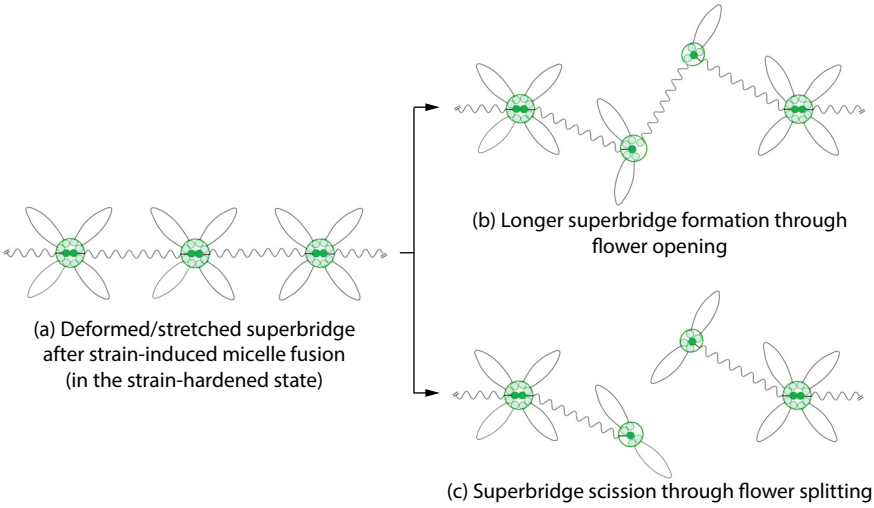

Fig. 12 Illustration of strain-induced structural changes of flower micelles in the superbridge backbone: (a) superbridge after the flower-micelle fusion, (b) flower micelle split into two smaller flower micelles that are still connecting the HEUR backbone; (c) fully split flower micelle that converts the superbridge into tails.

perbridge backbone; cf. Fig. 12(b). This opening-up process is similar to release of a fishing thread from a real of fishing rod, and in this sense the flower micelle serves as a storage box of the HEUR chain backbone. If the flower micelle is opened in this way but cannot stand with the superbridge tension, it would split into two smaller micelles; *cf.* Fig. 12(c). This flower splitting is a follow-up sequence of the flower opening (that destabilizes the small flowers), and is *assumed* to occur only for the opened-up flowers.

With the above assumptions, the shear stress on application of a step strain γ in x-direction is classified into several cases, as explained below.

For a case of no opening/splitting of flower micelles, the whole superbridge is affinely deformed to exhibit the shear stress expressed in the standard form for flexible Gaussian chains[34] as:

$$\sigma_0 = \kappa^{[N+1]}\left\langle R_x^{[N+1]} R_y^{[N+1]}\right\rangle_\gamma = \gamma k_B T \tag{3a}$$

where, $R_x^{[N+1]}$ and $R_y^{[N+1]}$ denote components of the end-to-end vector of **R** of the superbridge in the x and y directions (shear and shear gradient directions), $\langle ...\rangle_\gamma$ denotes the ensemble average in the affinely deformed state, and $\kappa^{[N+1]} = 3k_BT/\left\langle \{R^{[N+1]}\}^2\right\rangle_{eq}$ is an elastic strength of the superbridge determined by its equilibrium mean-square end-to-end distance $\left\langle \{R^{[N+1]}\}^2\right\rangle_{eq}$. The corresponding free energy, contributed from the elasticity of the superbridge affinely deformed to have the mean-square end-to-end distance $\left\langle \{R^{[N+1]}\}^2\right\rangle_\gamma = \left(1+\gamma^2/3\right)\left\langle \{R^{[N+1]}\}^2\right\rangle_{eq}$, is given by

$$F_0 = \frac{\kappa^{[N+1]}}{2}\left\langle \{R^{[N+1]}\}^2\right\rangle_\gamma = \frac{3k_BT}{2}\left(1+\frac{\gamma^2}{3}\right) \tag{3b}$$

For a case of opening (no splitting) of n flowers (*cf.* Fig. 12b), the backbone of superbridge is composed of $N + 1 + n$ HEUR chains, and n HEUR chains transferred from the flowers to the superbridge backbone are quickly equilibrated with $N + 1$ HEUR chains originally forming the superbridge backbone. After this equilibration, the stress and free energy can be expressed as:

$$\sigma_n^{[open]} = A_n \gamma k_B T \tag{4a}$$

$$F_n^{[open]} = \frac{3k_BT}{2}\left(1+\frac{\gamma^2}{3}\right)A_n + n\tilde{E}_{open}k_BT \tag{4b}$$

with

$$A_n = \frac{\kappa^{[N+n+1]}}{\kappa^{[N+1]}} = \frac{N+1}{N+n+1} \tag{5}$$

where the factor A_n specified by Eq. (5) is a ratio of the elastic strength of the superbridge backbone composed of $N + n + 1$ HEUR chains (after opening of n flowers) to the strength of the original superbridge backbone composed of $N + 1$ HEUR chains, and the factor $(3k_BT/2)(1 + \gamma^2/3)A_n$ appearing in Eq. 4(b) represents the elastic free energy of the superbridge backbone after the flower micelle opening. In Eq. 4(b), $\tilde{E}_{open}$ represents an energetic penalty of opening a flower micelle normalized by the thermal energy k_BT.

For a case of splitting n flowers (*cf.* Fig. 12c), the backbone connectivity of superbridge is lost to give $n + 1$ free chains (dangling tails and/or unconnected fragments of linear chains) not sustaining the connectivity of the associative network. The corresponding stress and free energy are straightforwardly expressed as:

$$\sigma_n^{[split]} = 0 \tag{6a}$$

$$F_n^{[split]} = \frac{3k_BT}{2}(n+1) + n\tilde{E}_{split}k_BT \tag{6b}$$

In Eq. (6b), the factor $3k_BT/2$ represents the elastic free energy of each free chain having an equilibrated Gaussian conformation, and $\tilde{E}_{split}$ is a normalized energetic penalty of splitting a flower micelle into two smaller micelles.

Here, we should emphasize that the flower micelle opening (Eqs. 4 and 5) has been included in the above formulation because of the softness of those micelles. The aggregates of salt groups serving as the dynamic crosslinks in SPS-Na ionomer are fragile, so that only the splitting (mechanical

breakage) was considered in the previous model for SPS-Na.[31]

Now, we attempt to calculate the averaged stress $\langle\sigma\rangle$ and averaged free energy $\langle F\rangle$ from Eqs. (3)–(6). For this purpose, we assume a local equilibrium among superbridges having intact, opened-up, and split flower micelles. In addition, we assume that the micelle opening (Fig. 12b) is a pre-requisite for the micelle splitting (Fig. 12c), namely, the opened-up and split micelles do not coexist in a given superbridge (the latter assumption corresponds to the soft and ductile feature of the alkyl aggregates in the HEUR solution). With these assumptions, the averages $\langle\sigma\rangle$ and $\langle F\rangle$ are simply expressed as

$$\frac{\langle\sigma\rangle}{\gamma k_B T} = P_0 + \sum_{n=1}^{N} A_n P_n^{[\mathrm{open}]} \tag{7}$$

$$\frac{\langle F\rangle}{k_B T} = \left(\frac{3}{2}+\frac{\gamma^2}{2}\right)P_0 + \sum_{n=1}^{N}\left\{A_n\left(\frac{3}{2}+\frac{\gamma^2}{2}\right)+n\tilde{E}_{\mathrm{open}}\right\}P_n^{[\mathrm{open}]} + \sum_{n=1}^{N}\left\{\frac{3}{2}(n+1)+n\tilde{E}_{\mathrm{split}}\right\}P_n^{[\mathrm{split}]} \tag{8}$$

The probabilities P appearing in Eqs. (7) and (8) are given in the Boltzmann form as

$$P_0 = \frac{1}{W}\exp\left(-\frac{3}{2}-\frac{\gamma^2}{2}\right) \tag{9a}$$

$$P_n^{[\mathrm{open}]} = \frac{1}{W}\frac{N!}{n!\,(N-n)!}\exp\left\{-A_n\left(\frac{3}{2}+\frac{\gamma^2}{2}\right)-n\tilde{E}_{\mathrm{open}}\right\} \tag{9b}$$

$$P_n^{[\mathrm{split}]} = \frac{1}{W}\frac{N!}{n!\,(N-n)!}\exp\left\{-\frac{3}{2}(n+1)-n\tilde{E}_{\mathrm{split}}\right\} \tag{9c}$$

$$W=\exp\left(-\frac{3}{2}-\frac{\gamma^2}{2}\right)+\sum_{n=1}^{N}\frac{N!}{n!\,(N-n)!}\exp\left\{-A_n\left(\frac{3}{2}+\frac{\gamma^2}{2}\right)-n\tilde{E}_{\mathrm{open}}\right\} + \sum_{n=1}^{N}\frac{N!}{n!\,(N-n)!}\exp\left\{-\frac{3}{2}(n+1)-n\tilde{E}_{\mathrm{split}}\right\} \tag{10}$$

Comparison of Model with Experiments

It should be noted that at the time of imposing the step strain γ, the number of HEUR chains per superbridge (N + 1) decreases, and thus the number density of the superbridges increases with increasing γ, due to strain-induced fusion of the flower micelles as noted from the strain-hardening at short t (*cf.* Fig. 4). This change of N, shown in Appendix A1, is not explicitly incorporated in Eqs. (7)–(10) formulated as above. Thus, we approximated N as an average value for large γ. Specifically, we adopted N=10 and 2 for the 1 wt% and 5 wt% HEUR solutions. In the future work, we plan to improve the above analysis for incorporating changes of N with γ.

Based on the above model analysis, and using plausible values of $\tilde{E}_{\mathrm{open}}$=2 and $\tilde{E}_{\mathrm{split}}$=4 (that allow thermal relaxation of the associative network within a reasonable time), we calculated the averaged stress $\langle\sigma\rangle$ and averaged free energy $\langle F\rangle$ as functions of the magnitude of the step strain γ. Fig. 13 compares the effective damping function deduced from the above model (blue curves), $h_{\mathrm{eff}}(\gamma) = \{\langle\sigma(\gamma)\rangle/\gamma\}/\{\langle\sigma(\gamma)\rangle/\gamma\}_{\gamma\to 0}$ calculated from Eq. (7) combined with Eqs. (9) and (10), with the $h_{\mathrm{eff}}(\gamma)$ data (circles; reproduced from Fig. 9). The corresponding increase of the average free energy, $\langle\Delta F(\gamma)/k_BT\rangle = \langle\{F(\gamma)-F(0)\}/k_BT\rangle$ calculated from Eqs. (8)–(10), is shown in Fig. 14.

Uniform deformation is considered to become unstable after the free energy increment exhibits a peak on an increase of γ as shown in Fig. 14, which is in the same situation as discussed for SPS-Na ionomer.[31] Plastic behavior characterized by a relationship $\langle\sigma(\gamma)\rangle/\gamma \propto 1/\gamma$ (*i.e.*, $\langle\sigma(\gamma)\rangle$ = constant) is supposed to emerge in this unstable zone. Correspondingly, in Fig. 13, the calculation from Eqs. (7), (9) and (10) (solid blue curve) is switched to the plastic behavior (dotted blue line).

Fig. 13 shows that the $h_{\mathrm{eff}}(\gamma)$ data of the HEUR solutions are considerably close to the calculated blue curve/line. This result suggests an importance of the flower micelle *opening* prior to the micelle splitting that results from soft, ductile feature of the aggregates of alkyl groups in the HEUR solutions. This point can be confirmed from comparison of the $h_{\mathrm{eff}}(\gamma)$ data and the thin green curve, the latter calculated with

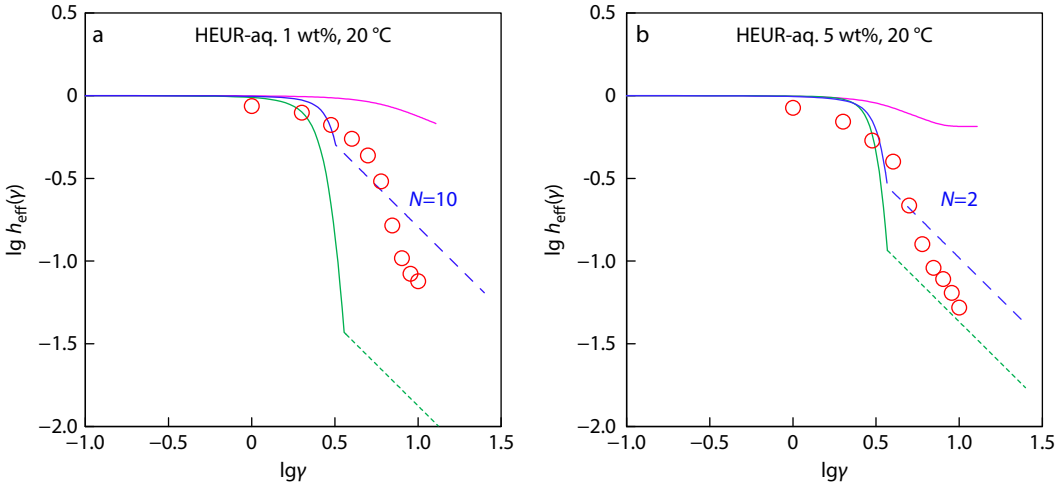

Fig. 13 Comparison of $h_{\mathrm{eff}}(\gamma)$ data (red circles) of HEUR solutions (reproduced from Fig. 9) with the model calculation based on Eqs. (7), (9) and (10). Panels (a) and (b) show the results for the solutions with c=1 wt% and 5 wt%, respectively. Blue solid and dotted curves show h_{eff} calculated in the stable and unstable zones of γ. Green and pink curves show $h_{\mathrm{eff}}(\gamma)$ calculated for the hypothetical cases of $P_n^{[\mathrm{open}]}$=0 (flower-micelle splitting without pre-opening) and $P_n^{[\mathrm{split}]}$=0 (lack of flower-micelle splitting).

https://doi.org/10.1007/s10118-026-3573-1

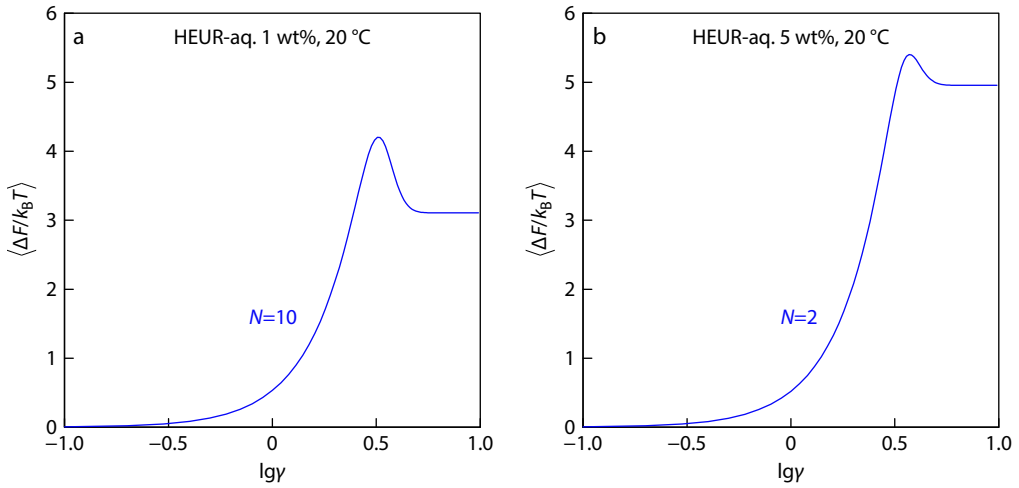

Fig. 14 Normalized free energy increment $\langle \Delta F/k_BT \rangle$ of the HEUR solutions defined with respect to undeformed state calculated through Eqs. (8)–(10). Panels (a) and (b) show the results for the solutions with c=1 wt% and 5 wt%, respectively. The uniform deformation becomes unstable after $\langle \Delta F/k_BT \rangle$ exhibits a peak.

$P_n^{[open]}$=0, namely, for the case of only micelle splitting without pre-opening. The deviation of the $h_{eff}(\gamma)$ data from the green curve, noted in particular for the 1 wt % HEUR solution, is indicative of the importance of the soft and ductile feature of the alkyl aggregates in the damping behavior of the HEUR solutions. This feature also leads to the relatively weak γ-dependence of $h_{eff}(\gamma)$.

In relation to this point, we remember that the $h_{eff}(\gamma)$ data of the HEUR solution (circles in Fig. 9) are a little larger, namely the effective damping is a little weaker, for c=1 wt% than for c=5 wt%. The model calculation also suggests this difference between c=1 wt% and 5 wt%, as most clearly noted from direct comparison of the calculated results for these c shown in Appendix A2. Thus, the number of HEUR chains in the superbridge backbone (N + 1 considered in the model) appears to be an important factor leading to the difference of $h_{eff}(\gamma)$ for c=1 wt% and 5 wt%.

We also remember that $h_{eff}(\gamma)$ data of the SPS-Na ionomer are close to the model calculation just considering the fracture/splitting of the salt aggregates,[31] not the aggregate opening. Thus, the nonlinear damping of the SPS-Na ionomers appears to be governed by the fragile property of the salt aggregates, which makes a contrast from the nonlinear behavior of the HEUR aq solutions contributed from the opening of the soft/ductile flower micelles.

CONCLUSIONS

For 1 wt% and 5 wt% aqueous solutions of telechelic HEUR forming transient networks formed through association of the $C_{16}H_{33}$ alkyl groups at the chain ends, a systematic investigation was conducted for the nonlinear stress relaxation behavior under step strain γ. The results revealed distinct time-dependent characteristics of the nonlinear relaxation modulus $G(t,\gamma)$. Pronounced strain hardening was observed at very short t, while the terminal relaxation at long t exhibited the time–strain separable damping (softening). The hardening of the HEUR solutions was rather weak in a sense that their short t modulus even under the largest strain examined (γ=10) stayed much smaller than the ideal modulus $G°$ expected for a perfectly dense network having individual HEUR chains as the network strands. This behavior was in contrast to the hardening of the previously examined SPS-Na ionomer[31] exhibiting $G(t,\gamma) \cong G°$ even at small γ (=2). Correspondingly, the γ dependence of the damping function $h(\gamma)$ characterizing the long-t softening was significantly weaker than that observed for SPS-Na ionomer. These features of the HEUR solutions suggested that the hydrophobic association of the alkyl groups of HEUR, resulting in flower micelle formation, was much weaker than the electrostatic association of the sodium sulfonate salt groups of the ionomers.

In double-step stress relaxation experiments wherein strains of the same magnitude were successively applied in the opposite directions within a very short interval of time, the HEUR solutions under the first strain exhibited hardening of their stress but also showed a large stress of the opposite sign remaining under the second strain. If the hardening of those solutions were mainly due to the FENE effect without changes in their transient network structure, the solutions should have behaved similarly to chemically crosslinked rubbers and the stress under the second strain should have essentially vanished. Thus, the large stress observed for the HEUR solutions under the second step strain indicated that the FENE effect was not the main structural origin of their hardening.

On the basis of this observation, the hardening of the HEUR solutions was attributed to the transient fusion of the flower micelles under large step strains that effectively increased the number density of the network strands thereby activating the strain-hardening: the core of those micelles, the associated alkyl groups at the HEUR chain ends, were in a molten liquid state and behaved as a ductile dynamic crosslink, so that the transient micellar fusion could have easily taken place. This structural change would be followed by splitting of the fused micelle into smaller micelles either being connected by the HEUR chain backbone or being fully separated. The former type of structural change results in the stress relaxation to a

https://doi.org/10.1007/s10118-026-3573-1

non-vanishing level, whereas the latter type leads to full relaxation of the stress. A simple model analysis considering the distribution of the number and length of the network strands formed on the fusion/splitting of the flower micelles described the magnitude of softening (damping) of the HEUR solutions at long t considerably well. This result also suggested that the much stronger damping observed for the SPS-Na ionomer[31] reflected brittleness of the associated sodium sulfonate salt groups that disturbed the opening of the salt aggregates without full breakage/separation.

On the basis of the above findings, we may situate the short-t hardening and the long-t softening as the universal feature of associative polymers. The magnitudes of hardening and softening should reflect the strength of the associative force and ductileness of the resulting associates (*e.g.*, flower micelles and/or salt aggregates). Quantitative description of the hardening/softening of the associative polymers in general, requiring full analysis of the mechanical characteristics of the associates (*e.g.*, ductile flower micelles and fragile salt aggregates), is considered to be an important subject of future work.

APPENDIX

Appendix A1: Estimation of Number of HEUR Chains in Superbridge

The ratio of the short-t modulus data to the ideal modulus, $G^\circ = cRT/M_{HEUR}$, is equivalent to the molecular weight ratio of the superbridge including the flowers to the HEUR chain:

$$G(\text{short } t, \gamma) = \frac{cRT}{M_{\text{superbridge}}(\gamma)} \text{ and}$$
$$G^\circ = \frac{cRT}{M_{HEUR}} \rightarrow \frac{G^\circ}{G(\text{short } t, \gamma)} = \frac{M_{\text{superbridge}}(\gamma)}{M_{HEUR}} \quad \text{(A1)}$$

where the $M_{\text{superbridge}}(\gamma)/M_{HEUR}$ ratio, evaluated from the $G(t,\gamma)$ data in Fig. 4, corresponds to the number of HEUR chains, $N' + 1$, in a superbridge including the flowers. The N' value estimated from the data in Fig. 4 is shown in Fig. A1. Assuming that about a half of the HEUR chains are in the flower micelle, we may have a rough estimate of the number N of flower micelles in the superbridge backbone, $N \sim N'/2$: $N \sim 10$ and 2 for the 1 wt% and 5 wt% HEUR solutions, respectively. This estimate of N was utilized in the analysis in the main text (*cf.* Eqs. 7–10).

Appendix A2: Direct Comparison of Model Calculation for HEUR Solutions with c=1 wt% and 5 wt%

Fig. A2 directly compares the effective damping function $h_{eff}(\gamma)$ of the HEUR solutions calculated for c=1 wt% and 5 wt%; see blue and red curves. (Respective curves are separately shown in Fig. 9.) We note that $h_{eff}(\gamma)$ calculated for γ>3 (lg γ>0.5), namely in the plastic zone explained for Fig. 14, is larger for c=1 wt%. The $h_{eff}(\gamma)$ data (circles) are larger for c=1 wt% than for c=5 wt% and are reasonably close to the model calculation. This result suggests that the difference in the HEUR chain number in the superbridge backbone (N+1 considered in the model) is the main factor giving the difference observed for those c: Larger the N+1 (for lower c), smaller the decrease ratio of the elastic constant of the superbridge on the micelle opening, $A = (N + 1)/(N + n + 1)$ specified by Eq. (5), which is in harmony with the experimentally observed damping weaker for smaller c. Nevertheless, further refinements of the model, for example, consideration of changes of N with γ (discussed in Appendix A1) and of elastically inert loops in the chain population distribution, are necessary for rigid conclusion for this factor.

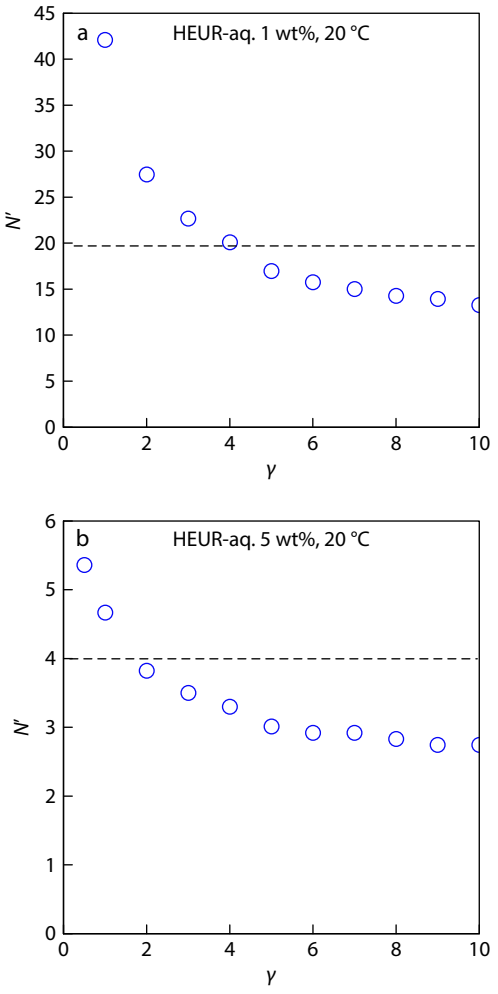

Fig. A1 The N' value of the solution with (a) c=1 wt% and (b) c=5 wt% estimated from the G° and $G(t,\gamma)$ data at short t in Fig. 4.

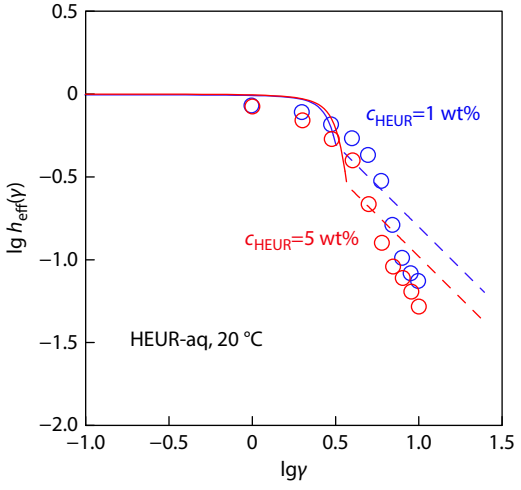

Fig. A2 Direct comparison of $h_{eff}(\gamma)$ data and model calculation for c=1 wt% and 5 wt%.

https://doi.org/10.1007/s10118-026-3573-1

Conflict of Interests

Quan Chen is an editorial board member for *Chinese Journal of Polymer Science* and was not involved in the editorial review or the decision to publish this article. All authors declare that thereare no competing interests.

Data Availability Statement

The data that support the findings of this study are available from the corresponding author upon reasonable request.

ACKNOWLEDGMENTS

This work was financially supported by the National Natural Science Foundation of China (Nos. 52425301 and 22173095).

REFERENCES

1 Annable, T.; Buscall, R.; Ettelaie, R.; Whittlestone, D. The rheology of solutions of associating polymers: Comparison of experimental behavior with transient network theory. *J. Rheol.* **1993**, *37*, 695–726.
2 Annable, T.; Buscall, R.; Ettelaie, R. Network formation and its consequences for the physical behaviour of associating polymers in solution. *Colloids Surf. A* **1996**, *112*, 97–116.
3 Xu, B.; Li, L.; Yekta, A.; Masoumi, Z.; Kanagalingam, S.; Winnik, M. A.; Zhang, K. W.; Macdonald, P. M. Synthesis, characterization, and rheological behavior of polyethylene glycols end-capped with fluorocarbon hydrophobes. *Langmuir* **1997**, *13*, 2447–2456.
4 Tam, K. C.; Jenkins, R. D.; Winnik, M. A.; Bassett, D. R. A structural model of hydrophobically modified urethane-ethoxylate (HEUR) associative polymers in shear flows. *Macromolecules* **1998**, *31*, 4149–4159.
5 Tripathi, A.; Tam, K. C.; McKinley, G. H. Rheology and dynamics of associative polymers in shear and extension: Theory and experiments. *Macromolecules* **2006**, *39*, 1981–1999.
6 Berret, J. F.; Séréo, Y.; Winkelman, B.; Calvet, D.; Collet, A.; Viguier, M. Nonlinear rheology of telechelic polymer networks. *J. Rheol.* **2001**, *45*, 477–492.
7 Berret, J. F.; Séréro, Y. Evidence of shear-induced fluid fracture in telechelic polymer networks. *Phys. Rev. Lett.* **2001**, *87*, 048303.
8 Ma, S. O. X.; Cooper, S. L. Shear thickening in aqueous solutions of hydrocarbon end-capped poly(ethylene oxide). *Macromolecules* **2001**, *34*, 3294–3301.
9 Pellens, L.; Corrales, R. G.; Mewis, J. General nonlinear rheological behavior of associative polymers. *J. Rheol.* **2004**, *48*, 379–393.
10 Pellens, L.; Ahn, K. H.; Lee, S. J.; Mewis, J. Evaluation of a transient network model for telechelic associative polymers. *J. Non-Newtonian Fluid Mech.* **2004**, *121*, 87–100.

Graphical Abstract

Nonlinear Stress Relaxation of End-associative Hydrophobically Modified Ethoxylated Urethane (HEUR) Solutions under Step Strain

Yu-Xuan Pei, Quan Chen, and Hiroshi Watanabe

Changchun Institute of Applied Chemistry, Chinese Academy of Sciences, China; University of Science and Technology of China, China; Kyoto University, Japan

Nonlinear softening factor h_{eff} of hydrophobically modified ethoxylated urethane (HEUR)-aq. solutions at long times, defined with respect to short-time hardened state, is considerably well described by a simple model formulating strain-induced HEUR micelle fusion followed by micelle opening/splitting associated with a free energy increase $\langle \Delta F/k_BT \rangle$ under strain.

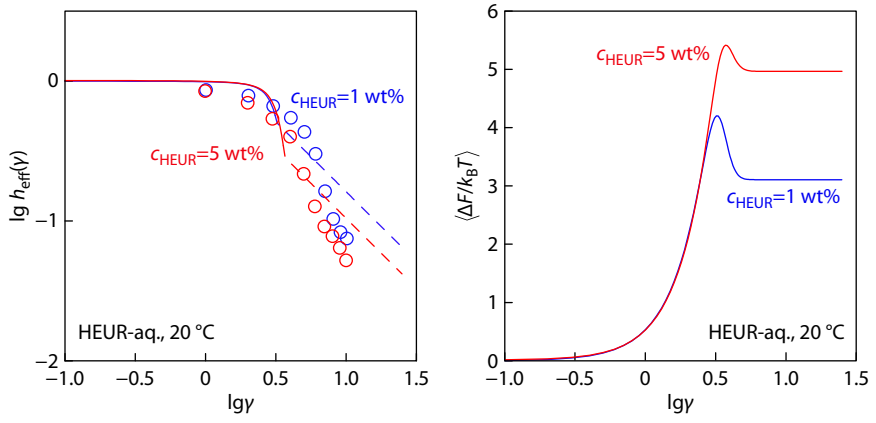

Chinese J. Polym. Sci. 2026, 44, 1790–1803 *https://doi.org/10.1007/s10118-026-3573-1*

11 Pellens, L.; Vermant, J.; Mewis, J. Deviations from the stress-optical rule in telechelic associative polymer solutions. *Macromolecules* **2005**, *38*, 1911–1918.
12 Suzuki, S.; Uneyama, T.; Inoue, T.; Watanabe, H. Nonlinear rheology of telechelic associative polymer networks: Shear thickening and thinning behavior of hydrophobically modified ethoxylated urethane (HEUR) in aqueous solution. *Macromolecules* **2012**, *45*, 888–898.
13 Uneyama, T.; Suzuki, S.; Watanabe, H. Concentration dependence of rheological properties of telechelic associative polymer solutions. *Phys. Rev. E* **2012**, *86*, 031802.
14 Suzuki, S.; Uneyama, T.; Watanabe, H. Concentration dependence of nonlinear rheological properties of hydrophobically modified ethoxylated urethane aqueous solutions. *Macromolecules* **2013**, *46*, 3497–3504.
15 Marrucci, G.; Bhargava, S.; Cooper, S. L. Models of shear-thickening behavior in physically crosslinked networks. *Macromolecules* **1993**, *26*, 6483–6488.
16 Tanaka, F.; Edwards, S. F. Viscoelastic properties of physically crosslinked networks. 1. Transient network theory. *Macromolecules* **1992**, *25*, 1516–1523.
17 Tanaka, F.; Koga, T. Nonaffine transient network theory of associating polymer solutions. *Macromolecules* **2006**, *39*, 5913–5920.
18 Koga, T.; Tanaka, F.; Kaneda, I.; Winnik, F. M. Stress buildup under start-up shear flows in self-assembled transient networks of telechelic associating polymers. *Langmuir* **2009**, *25*, 8626–8638.
19 Koga, T.; Tanaka, F. Theoretical predictions on normal stresses under shear flow in transient networks of telechelic associating polymers. *Macromolecules* **2010**, *43*, 3052–3060.
20 Indei, T.; Koga, T.; Tanaka, F. Theory of shear-thickening in transient networks of associating polymer. *Macromol. Rapid Commun.* **2005**, *26*, 701–706.
21 Ahmadi, M.; Hawke, L. G. D.; Goldansaz, H.; van Ruymbeke, E. Dynamics of entangled linear supramolecular chains with sticky side groups: influence of hindered fluctuations. *Macromolecules* **2015**, *48*, 7300–7310.
22 Hu, X. B.; Vatankhah-Varnoosfaderani, M.; Zhou, J.; Li, Q. X.; Sheiko, S. S. Weak hydrogen bonding enables hard, strong, tough, and elastic hydrogels. *Adv. Mater.* **2015**, *27*, 6899–6950.
23 Scherz, L. F.; Costanzo, S.; Huang, Q.; Schlütter, A. D.; Vlassopoulos, D. Dendronized polymers with ureidopyrimidinone groups: An efficient strategy to tailor intermolecular interactions, rheology, and fracture. *Macromolecules* **2017**, *50*, 5176–5187.
24 Zhang, Z. J.; Liu, C.; Cao, X.; Gao, L. C.; Chen, Q. Linear viscoelastic and dielectric properties of strongly hydrogen-bonded polymers near the sol-gel transition. *Macromolecules* **2016**, *49*, 9192–9202.
25 Parisi, D.; Ditillo, C. D.; Han, A. J.; Lindberg, S.; Hamersky, M. W.; Colby, R. H. Rheological investigation on the associative properties of poly(vinyl alcohol) solutions. *J. Rheol.* **2022**, *66*, 1141–1150.
26 Chassenieux, C.; Tassin, J. F.; Gohy, J. F.; Jérôme, R. Elongation of telechelic ionomers under shear: a rheological and rheo-optical study. *Macromolecules* **2000**, *33*, 1796–1800.
27 Qiao, X.; Weiss, R. A. Nonlinear rheology of lightly sulfonated polystyrene ionomers. *Macromolecules* **2013**, *46*, 2417–2424.
28 Chen, Q.; Huang, C.; Weiss, R. A.; Colby, R. H. Viscoelasticity of reversible gelation for ionomers. *Macromolecules* **2015**, *48*, 1221–1230.
29 Huang, C.; Chen, Q.; Weiss, R. A. Rheological behavior of partially neutralized oligomeric sulfonated polystyrene ionomers. *Macromolecules* **2017**, *50*, 424–431.
30 Zhang, Z. J.; Chen, Q.; Colby, R. H. Dynamics of associative polymers. *Soft Matter.* **2018**, *14*, 2961–2977.
31 Pei, Y. X.; Chen, Q.; Matsumiya, Y.; Watanabe, H. Nonlinear relaxation of unentangled associative polymers: strain-induced hardening and softening. *Macromolecules* **2025**, *58*, 953–967.
32 Kawaguchi, S.; Imai, G.; Suzuki, J.; Miyahara, A.; Kitano, T.; Ito, K. Aqueous solution properties of oligo- and poly(ethylene oxide) by static light scattering and intrinsic viscosity. *Polymer* **1997**, *38*, 2885–2891.
33 Wagner, H. L. The Mark-Houwink-Sakurada equation for the viscosity of atactic polystyrene. *J. Phys. Chem. Ref. Data* **1985**, *14*, 1101–1106.
34 Watanabe, H. Viscoelasticity and dynamics of entangled polymers. *Prog. Polym. Sci.* **1999**, *24*, 1253–1403.

https://doi.org/10.1007/s10118-026-3573-1